Available online freely at www.isisn.org

Bioscience Research

Print ISSN: 1811-9506 Online ISSN: 2218-3973

Journal by Innovative Scientific Information & Services Network

RESEARCH ARTICLE BIOSCIENCE RESEARCH, 2023 20(3):850-858. **OPEN ACCESS**

Evaluation of DNA and Histological changes in the liver of Albino Rats treated with Silver Nanoparticles

Lamiaa Elsayed Mokhtar Deef[1*], Kadry Elbakry[1], Nahed Ahmed Omar[1], Shereen Ahmed Fahmy[1] and Abdullah Hamad Yaquob Abduljalil[2]

[1]Department of Zoology, Faculty of Science, Damietta University, New Damietta, Damietta, **Egypt**
[2]Department of Zoology, Faculty of Science, Sebha University, Sebha, **Libya**

***Correspondence:** lamiaadeef@yahoo.com **Received 14 July 2023, Revised: 21 Sep., 2023, Accepted: 22 Sep., 2023 e-Published: 25 Sep., 2023**

Silver nanoparticles (AgNPs) are widely used in industrial and medical applications. However, there is a growing concern about the potentialities of AgNPs to induce genotoxicity and DNA damage in humans. Mutations in mitochondrial DNA cause a number of neurological diseases with defined neuropathology; however, mutations in this genome have also been found to be important in a number of more common neurodegenerative diseases. In this study, we discuss the importance of mitochondrial DNA mutations and speculate how such mutations could lead to cell loss. The present study aimed to indicate the harmful toxic effects caused by acrylamide (ACR) on mitochondrial gene from liver of rats and the possible protective role of silver nanoparticles derived from *Moringa oliefera* leaves against toxic effects of ACR. Thirty adult male albino rats were used for three weeks and randomly divided into six groups. Partial sequences for the mitochondrial COI gene in the six groups were determined. Direct sequencing shows some changes in DNA sequence for mutated samples in comparison with the negative control group using forward and reverse primers. The treatment of acrylamide-injured rats with silver nanoparticles of *Moringa oleifera* ameliorate the histopathological changes induced by acrylamide.

Keywords: Acrylamide, Nanoparticles, liver, rats, histology

INTRODUCTION

Food products derived from raw materials that are low in proteins, rich in carbohydrates, and heat treated at high temperatures (>120°C), are the main source of acrylamide (ACR), which has been shown to have carcinogenic effects in animals, causing genotoxicity, neurotoxicity, and reproductive toxicity. For this reason, acrylamide may have neurotoxic effects on humans (Ahn et al. 2002; Jamshidi, 2015). According to several research, humans consume between 0.3 and 0.6 g/kg of body weight of ACR on a daily average. Children and teenagers are more at risk than other age groups due to their propensity to consume more foods containing acrylamide, such as French fries, chips, and crackers (Kadawathagedara et al. 2018). After exposure to acrylamide via ingestion, inhalation, or intradermally, accumulation is highest in concentration in the blood than in any other tissues (Shipp et al. 2006).

It has also been shown that ACR can be metabolized into glycidamide via the cytochrome P450 pathway. This can then form a DNA-reactive epoxide that may induce changes in the signal pathway and cellular function (Törnqvist, 2005).

Mitochondria are the only organelles (other than the nucleus) with their own DNA, which is maternally inherited (Giles et al. 1980; Ingman et al. 2000). The mammalian mitochondrial DNA (mtDNA) is a circular, double-stranded DNA that lacks introns and has only 7% noncoding sequences in contrast to the genomic DNA (Fernandez-Silva et al. 2003). The mtDNA encodes 37 genes, including 13 protein-coding genes that, in conjunction with subunits encoded by the nuclear genome, form the electron transport chain, the primary ATP producer for the cell. MtDNA has a mutation rate of 10–20 times that of nuclear DNA, probably because of a failure of proofreading by mtDNA polymerases and lack of an effective repair system (DiMauro and Schon, 2003; Mason and Lightowlers, 2003; Finsterer, 2004; Lynch et al. 2006). Hundreds of mutations in the tRNA, rRNA, and protein coding genes as well as in the D-loop of the human mitochondrial genome are associated with disease (Brandon et al. 2005). Interestingly,15% of known human diseases related to mutations in the mitochondria are found within the tRNA genes (http://www.mitomap.org). Due to its extensive physiological characterization along with the ability to be genetically manipulated (Akaneya et al. 2005; Charron et al. 2005; Chen and Wang, 2005; Ng and Krolewski, 2005;

Van Dijk et al. 2005), the rat is a useful model for many different complex diseases.

Cytochrome c oxidase I (COX1) also known as mitochondrially encoded cytochrome c oxidase I (MT-CO1) is a protein that in humans is encoded by the MT-CO1 gene. In other eukaryotes, the gene is called COX1, CO1, or COI (Kosakyan et al. 2012). Cytochrome c oxidase I is the main subunit of the cytochrome c oxidase complex. Mutations in MT-CO1 have been associated with Leber's hereditary optic neuropathy (LHON), acquired idiopathic sideroblastic anemia, Complex IV deficiency, colorectal cancer, sensorineural deafness, and recurrent myoglobinuria. One of 37 mitochondrial genes, the MT-CO1 gene is located from nucleotide pairs 5904 to 7444 on the guanine-rich heavy (H) section of mtDNA. The gene product is a 57 kDa protein composed of 513 amino acids. Cytochrome c oxidase subunit I (CO1 or MT-CO1) is one of three mitochondrial DNA (mtDNA) encoded subunits (MT-CO1, MT-CO2, MT-CO3) of respiratory complex IV. Complex IV is the third and final enzyme of the electron transport chain of mitochondrial oxidative phosphorylation (Zong et al. 2013).

Moringa oleifera is one of the Brassica order and belongs to the Moringaceae family, a single genus of approximately thirteen species (Mahmood et al. 2010). In tropical and subtropical countries, Moringa (*Moringa oleifera*) has become common as a native Indian medicinal herb (Fahey, 2005). Numerous studies have shown that *Moringa oleifera* leaves and seed extract are effective antioxidants that protect against the harmful effects of free radical attack and oxidative stress (Prakash et al. 2007).

In addition, *Moringa oliefera* is rich in a variety of essential phytochemicals (enzymes) such as catalase, polyphenol oxidase, ascorbic acid oxidase, total phenols, and vitamins. Interestingly, it has been shown that the antioxidant efficiency of *Moringa oliefera* leaf extract, which is rich in phytoconstituents, can be enhanced by incorporating silver nanoparticles (Ag-NPs) (Aboulthana et al. 2021). Silver nanoparticle applications in different areas, such as chemistry, pharmaceuticals, electronics, and catalysis, are well known. Silver nanoparticles can be produced using different methods.

Among these, biological methods for their synthesis are environmentally friendly, as non-toxic chemicals are used in their production. More specifically, plant extracts, proteins, enzymes, triglycerides, antioxidants, glycoproteins, flavonoids, terpenes, and tannins are used to reduce and stabilize the nanoparticles (Ramaswamy et al. 2019). The purpose of this study is to indicate whether there are harmful toxic effects caused by acrylamide on COI gene and to determine the possible protective role of silver nanoparticles derived from *Moringa oliefera* leaves against the toxic effect of ACR.

MATERIALS AND METHODS

Chemicals and Plant Materials

The acrylamide (ACR) used for this study was obtained from Sigma Chemical Company, England, UK. Fresh, loose leaves of *Moringa oliefera* plant (Family: Moringaceae) were collected from Damietta City, Egypt and were identified and confirmed by the Botany Department of Damietta university. The leaves were washed three times using distilled water, then dried and ground into powder.

Animals and their Housing

The current study was conducted on 30 adult male Wester albino rats. The weight of each rat was approximately 150 grams, and they were purchased from Helwan Animal Station. The animals were housed in separate cages (five rats in each according to their experimental groupings) and were subjected to cycles of 12 hours light / 12 hours dark at 25±2 °C. They were acclimatized for 14 days before the experiments began and were allowed free access to food and water under the standard conditions dictated by the Animal Ethics Committee at Damietta University.

Preparation of Moringa oleifera Extract

The *Moringa oleifera* Extract was prepared by adding 10 grams of powder to 100mL of distilled water. This was subsequently mixed to dissolve the powder, which was then boiled for 10 minutes until the colour of the extracted solution changed to a light green colour. The extract was filtered through filter paper and stored at 4 °C for future use as *Moringa oleifera* leaf extract (MO) (Ghosh et al. 2014; Abdel-Rahman et al. 2022).

Synthesis of Silver Nanoparticles Carried by Moringa oleifera (MO-NPs)

In this experiment, 10mL of MO-extract was added to 190mL of 2mM silver nitrate solution with continuous stirring. In order for the solution to turn dark brown, the mixture is stirred in a magnetic stirrer at room temperature for four hours and then incubated in the dark for 24 hours. At the same temperature, the solution was centrifuged at 5000 rpm for at least 20 minutes to allow the solution to condense into pellets. The supernatant was then discarded, and the granules were re-dispersed in distilled water and left to dry at a room temperature before being stored for future use (Ghosh et al. 2014; Abdel-Rahman et al. 2022).

Experimental Design

The rats were randomly divided into six groups of equal numbers (five rats per each) as follows:

Control group (CT group): rats received nothing additional to their normal diet.

Acrylamide group (ACR group): rats were given 50 mg/kg body weight in their drinking water daily for three weeks (LoPachin et al. 2006; Gawesh et al. 2021).

Silver nanoparticles of *Moringa oleifera* group (MO-NPs group): rats received 50 mg/kg body weight of MO-NPs daily for three weeks (Malathi et al., 2018; Ramaswamy et al., 2019).

Acrylamide + MO-NPs group (ACR+MO-NPs group): rats were given 50 mg/kg body weight of acrylamide and received MO-NPs 50 mg/kg body weight orally, daily, for three weeks (Malathi et al. 2018; Ramaswamy et al. 2019).

Protection group (MO-NPs/ACR group): rats received 50 mg/kg body weight of MO-NPs daily for three weeks and were given 50 mg/kg body weight of acrylamide daily for three weeks.

Treatment group (ACR/MO-NPs group) (ACR for 3 weeks followed by MO-NPs for 3 weeks).

Histological study:

Following animal sacrifice, liver tissues were gathered, fixed in 10% formalin, processed according to standard procedure, and then embedded in paraffin. For microscopic analysis, 5 µm thick slices were cut and stained with hematoxylin and eosin (H&E) dye (Drury et al. 1976). A light microscope was used to view and take pictures of the stained sections.

Molecular study

A total of 30 samples were included, Samples of liver tissues from all studied species were taken immediately and frozen at - 80 ºC. A GeneJET™ kit Genomic DNA Kit K0721 was used to extracting of DNA. The COI gene was amplified using thermocycler. Pairs of primers, Rn-F CGG CCA CCC AGA AGT GTA CAT C Rn-R GGC TCG GGT GTC TAC ATC TAG G were used to target the COI gene of 352 bp size. DNA barcode cycling conditions: One cycle of 95° C for 5 min; 30 cycles of 95°C for 30 s, 45°C for 15 s, 72°C for 30 s; 1 cycle of 72°C for 7 min; and indefinite hold at 4°C.The polymerase chain reaction (PCR) thermal program was set as described by Khalifa et al. (2018).

PCR products were investigated by running in a 2.0% agarose gels and stained with ethidium bromide. Successful PCR bands were cut out and purified using the QIAquick PCR purification kit from Quiagen®. The clean PCR products were sequenced using an automated sequencer following the manufacturer's protocols.

Genetic data analysis

All mtDNA nucleotide sequences were aligned by using the Clustal W software and identical sequences were considered as the same haplotype. MEGA 7.0.14 software (Kumar et al. 2016) was used to build phylogenetic tree based on a Maximum Likelihood analysis of complete COI gene sequences.

Basic Local Alignment Search Tool (BLAST)

To investigate and recognize created sequences, each was blast searched as a request through NCBI (National Center for Biotechnology Information) Blastn tool (www.ncbi.nlm.nih.gov/BLAST/).

RESULTS

Sequence variation using (COI)

In this study, partial sequences for the mitochondrial COI gene in the six groups were determined. The average A+T content was 48.9% which was smaller than the C+G content which was 51.1%. The aligned sequences length, A+T contents, C+G contents for each group and their average, were illustrated in (Table 1).

Moreover, the average nucleotide frequencies are 30.1% (A), 18.8% (T/U), 18.9% (C) and 32.2% (G). The percent composition of nucleotide varied from 29.1% to 30.6% (A), 18.1% to 19.5% (T), 18.2% to19.4 % (C), and 31.5%to 33.3% (G), which infers that studied group, are C and T poor and rich in G, A (Table 1).

Table 1: Percentage composition of nucleotides A, T, G, C, AT and GC in studied rats' groups

group	A%	T%	G%	C%	A+T%	C+G%
CT group	30.6	18.8	31.6	19.1	49.4	50.7
ACR group	30.4	18.5	33.3	18.2	48.9	51.5
MO-NPs group	29.1	19.5	32.8	18.5	48.6	51.3
ACR+MO-NPs group	30.4	18.1	32.2	19.3	48.5	51.5
MO-NPs /ACR group	29.9	19.2	32.1	18.9	49.1	51
ACR/ MO-NPs group	29.9	19.1	31.5	19.4	49	50.9
Mean	30.1	18.8	32.2	18.9	48.9	51.1

Table 2:Total genetic distance between the studied rats' groups.

	CT group	ACR group	MO-NPs group	ACR+MO-NPs group	MO-NPs /ACR group	ACR/ MO-NPs group
CT group	0					
ACR group	0.244	0				
MO-NPs group	0.017	0.259	0			
ACR+MO-NPs group	0.014	0.249	0.014	0		
MO-NPs /ACR group	0.010	0.249	0.017	0.014	0	
ACR/ MO-NPs group	0.014	0.254	0.014	0.007	0.010	0

The content of pyrimidine was smaller than that of purine. These values showed a weak A + T(48.9 %) to G + C (51.1%) asymmetry in nucleotide composition (Table 1). The maximum AT content was found in control group (49.4%) and the minimum in ACR+MO-NPs (48.5 %). The maximum and minimum GC contents were observed in Acrylamide group (ACR) (51.5%) and control group (CT) (50.7%) respectively.

The genetic distances among the groups ranged from 0.007 to 0.259. The highest genetic distance (0.259) found between Acrylamide group (ACR) and MO-NPs group which reflected the genetic effects of both Acrylamide and MO-NPs. While the lowest value (0.007) found between ACR+MO-NPs group and ACR/ MO-NPs group (Table 2).

The phylogenetic analysis among the four groups was achieved through Neighbour Joining method and revealed that Acrylamide group (ACR) group formed a separate cluster, while the remaining groups found in one clad within it, Control group (CT) and MO-NPs /ACR group formed a sister clade. ACR+MO-NPs group formed a another sister clade with ACR/ MO-NPs group (Fig. 1).

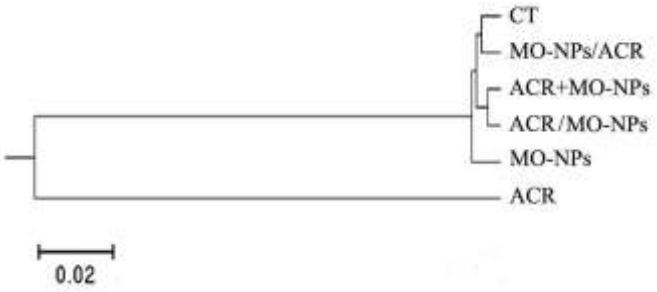

Figure 1: Phylogenetic tree using the Neighbour Joining method among the six groups based on partial sequences of COI gene. **Control group (CT), (MO-NPs/ACR) group; MO-NPs for three weeks then ACR for another three weeks; ACR+MO-NPs group; ACR+MO-NPs together for three weeks at the same time. (ACR/ MO-NPs) group; ACR for three weeks then MO-NPs for another three weeks. MO-NPs group; MO-NPs for three weeks. Acrylamide group; ACR for three weeks.**

Mutated PCR samples were subjected to sequencing to detect the point of mutation. Direct sequencing shows some changes in DNA sequence for mutated samples in comparison with the negative control group using forward (Fig. 2) and reverse primers.

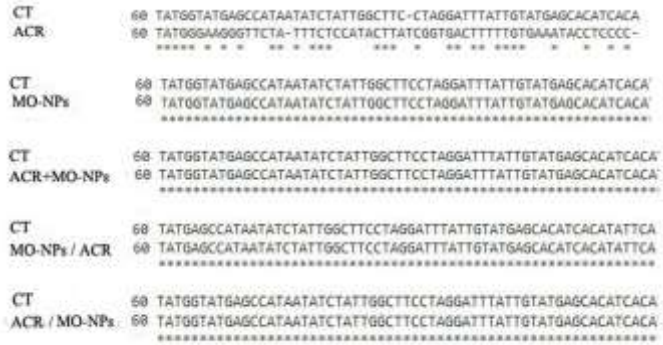

Figure 2: COI sequences of studied groups showing type of mutation. Control group (CT), Acrylamide group; ACR for three weeks. **MO-NPs group; MO-NPs for three weeks. ACR+MO-NPs group; ACR+MO-NPs together for three weeks. Protection group (MO-NPs/ACR); MO-NPs for three weeks then ACR for another three weeks at same time, (ACR/ MO-NPs) group; ACR for three weeks then MO-NPs for another three weeks.**

The most frequent type of mutation was simple bp substitution. All mutants obtained from control and the other groups were analyzed for sequence alterations in the COI gene. At least one base pair substitution, or deletion was detected in each mutant (Fig. 2).

Histological studies

Histopathological of liver in control group

Liver sections from control rats showed normal hepatic tissue structure and no obvious pathological changes. Hepatocytes are arranged in cords rayout from central veins to the portal areas and isolated by sinusoids. Hepatocytes have central vesicular nuclei with eosinophilic cytoplasm. Some cells have binucleated nuclei. Blood sinusoids contain Kupffer cells (Fig. 3A)

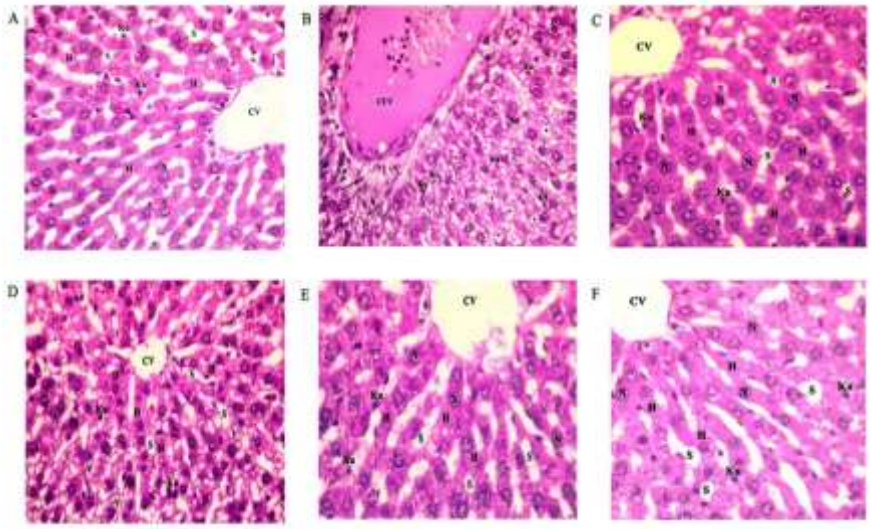

Figure 3: A photomicrograph of rat liver of control group showing preserved liver architecture. A: CV: central vein, H: hepatocyte, N: nucleus, Ku: kupffer cells, S: sinusoid. B: photomicrograph of the rat liver of the acrylamide-treated group. Showing the CCV: congested central vein, Ku: kupffer cells, *: necrosis, black arrow: inflammatory cells infiltration, head arrow: vacuolated cytoplasm. C: photomicrograph of the rat liver of the silver nanoparticles of *Moringa oleifera*-treated group. Showing the CV: central vein, H: hepatocyte, N: nucleus, Ku: kupffer cells, S: sinusoid. D: photomicrograph of the rat liver of the silver nanoparticles of *moringa oleifera* + ACR-treated group. Showing the CV: central vein, H: hepatocyte, N: nucleus, Ku: kupffer cells, S: sinusoid, V: vacuolated cytoplasm. E: photomicrograph of the rat liver of the silver nanoparticles of *Moringa oleifera*-protected group. Showing the CV: central vein, H: hepatocyte, N: nucleus, Ku: kupffer cells, S: sinusoid. F: photomicrograph of the rat liver of the silver nanoparticles of *Moringa oleifera*-treatment group. Showing the CV: central vein, H: hepatocyte, N: nucleus, Ku: kupffer cells, S: sinusoid. H&E X400

Histopathological of liver in Acrylamide (ACR) group

Treatment with acrylamide resulted in congestion of the central vein, necrosis of some hepatocytes, vacuolation of the cytoplasm, loss of the cellular boundaries of the hepatocytes, activation and increased number of kupffer cells, and infiltration with inflammatory cells.

The internal structure of the livers of the rats given the ACR treatment was drastically altered, as seen in Figure (3B), and these changes included significant edoema, intracytoplasmic vacuolization of hepatocytes, as well as inflammatory cell infiltration (Fig. 3B).

Histopathological of liver in Silver nanoparticles of *Moringa oleifera* group (MO-NPs group)

The liver of the silver nanoparticles of *Moringa oleifera*-treated group has a normal hepatic architecture, hepatocytes are normal in shape and size with clear nuclei (Fig. 3C).

Histopathological of liver in Silver nanoparticles of *Moringa oleifera* + ACRgroup (ACR+MO-NPs group)

In this group the silver nanoparticles of *Moringa oleifera* have moderately ameliorate the toxic effects induced by acrylamide indicated by vacuolated cytoplasm. The existence of normal periportal hepatic cells in the liver when the cells were stained with hematoxylin and eosin revealed a considerable improvement in the structure of the liver tissues when silver nanoparticles from *Moringa oleifera* were added to rats that had received an injection of ACR (Fig. 3D).

Histopathological of liver in protection group (silver Nanoparticles of *Moringa oleifera*for 3 weeks followed by ACR for 3 weeks (MO-NPs / ACR))

The pre-treatment of acrylamide-injured rats with silver nanoparticles of *Moringa oleifera* moderately ameliorate the histopathological changes induced by acrylamide. Slight blood congestion was recorded A section of the liver from the rats treated with silver nanoparticles of *Moringa oleifera* followed by ACR showed some of the blood congestion in some sinusoids, as can be seen from the reduced post-translational hypertrophy of the epithelium lining the bile duct and the normal periportal hepatocytes in the liver stained with hematoxylin and eosin stain (Fig. 3E).

Histopathological of liver in treatment group (ACR for 3 weeks followed by silver nanoparticles of *Moringa oleifera* for 3 weeks (ACR / MO-NPs)

The treatment of acrylamide-injured rats with silver nanoparticles of *Moringa oleifera* ameliorate the histopathological changes induced by acrylamide, the

hepatocytes arranged normally in cords, decreased inflammatory cells. Hematoxylin and eosin staining revealed normal hepatocytes and a thin layer of periportal fibrous connective tissue, with no signs of pathological damage (Fig. 3F)

DISCUSSION

Acrylamide (ACR) is a well-known environmental pollutant, which exerts a variety of systemic toxic effects on human beings following either occupational or dietary exposure (Baskar and Aiswarya, 2018). More importantly, the well-being of the public is being adversely affected by the intake of dietary ACR that is formed during heating processes of tobacco and carbohydrate-rich foods at high temperatures (Baskar and Aiswarya, 2018). So far, in addition to its high-profile nephrotoxicity, reproductive toxicity, and carcinogenicity (Exon, 2006), other toxic effects of ACR, for example, hepatotoxicity (Rizk et al. 2018) and neurotoxicity (Bo et al. 2018), have had more attention paid to them.

Acrylamide is a neurotoxic chemical and can cause peripheral and central neuropathy in humans and laboratory animals (LoPachin, 2004). The interference of ACR and its metabolite glycidamide (GA) with kinesin motor proteins in neurofilaments causes failure of the transport of nerve signals between axons, and this may be one of the mechanisms involved in its neurotoxicity (Sickles et al. 2007).

The results of COI sequences revealed that acrylamide caused genotoxicity comparing to the control group. The acrylamide treated group was genetically distance from the control group because of the effect of acrylamide. Several studies confirmed these findings; Manjanatha et al. (2006) reported that the high exposure concentrations of GA were mutagenic in some genes of liver.

The results of COI sequences showed the lowest distance value (0.007) was found between ACR+MO-NPs group and treatment group (ACR/ MO-NPs). This refers to improvement effect of Nano which decrease the effects of ACR.

In the present work, the treatment of the sample exposure to Nano particles with acrylamide doses led to more genotoxicity and DNA damage. The genetic distance between control group and protection treated group (MO-NPs/ACR) was very small (0.010). This reflected the effect of Nano particles on the genetic structure. Because synergistic or inhibitory effects, cascade, and indirect mechanisms can both reinforce or curb the expected responses from specific pollutants. Therefore, the biological consequences of chemical mixtures require delicate evaluation (Regoli et al. 2005).

The genetic distance between ACR+MO-NPs group and treatment group (ACR/ MO-NPs) was also very small (0.007). They were clustered together as a sister group. This reflected the effect of Nano particles on the genetic structure.

The ability of the newly created Nanoplatform to protect the liver from the degenerative changes that are caused may be the cause of its hepatoprotective effects. In comparison to other groups, the control group typically exhibited normal liver tissue, while in (MO-NPs drug supplement). In the current investigation, rat liver slices from the acrylamide-treated group showed altered hepatic parenchymal architecture, clear signs of liver cell senescence, including congestion and enlargement of the central vein and hepatic sinusoids. The hepatocytes had clear signs of degeneration in the form of pyknotic nuclei and cytoplasmic swelling. The Von Kupffer cells that line the sinusoids seemed dilated and crowded with necrotic alterations. Our results corroborated those of El-Bohi et al. (2011) who noted similar degenerative changes in the liver sections of acrylamide-treated rats, including edoema, hepatic cell degeneration, and hepatic sinusoidal cell enlargement.

Furthermore, Rahangadale et al. (2012) showed features of hepatic cell damage in the form of degeneration and pyknosis of the nuclei of the lining epithelium of some hepatic cells with pyknotic nuclei was seen in liver sections of acrylamide-treated rats. Sahai (2012), also mentioned similar degeneration and necrosis characterized by hydropic degeneration of certain hepatocytes and hypotrophied Kupffer cells. Other results showed that ACR produced ROS, which promoted the synthesis of lipid peroxidase. Cellular fatty acids are easily oxidised by ROS to produce lipid peroxyl radicals and lipid hydroxides (Al-Serwi and Ghoneim, 2015).

The improvement of the histopathological changes in the rat liver tissues after treatment of silver nanoparticles of *Moringa oleifera* (MO-NPs, MO-NPs + ACR, Protection group MO-NPs/ACR, and treatment group ACR/ MO-NPs rats). Liver tissue demonstrated a significant improvement following 3 weeks of therapy with silver nanoparticles from *Moringa oleifera,* as evidenced by a reduction in the degree of liver hyperplasia. In the current study was most likely brought on by the antioxidant effect of the silver nanoparticles of *Moringa oleifera* against oxidative damage in the liver.

Only a few reversible degenerative alterations, such as diffuse hydropic hepatocyte degeneration in the hepatic parenchyma, were visible after drug treatment in the MO-NPs + ACR, Protection group MO-NPs/ACR, and treatment group ACR/ MO-NPs rats. These findings were in agreement with those of Ezejindu et al. (2014), they claimed that rats given *Moringa oleifera* alone displayed normal cellular architecture under a light microscope with no notable differences from the control group. A chemical is deemed non-toxic to the hepatocytes when it has no effect on the amount of liver transaminases, which are significantly elevated in the blood in the event that the liver cells suffer from substantial necrosis (Senthilkumar et al. 2014). Because phenolic compounds exhibited substantial antioxidant activity, it was demonstrated that the mechanism of the hepatoprotective effect was

connected to the scavenging free radicals (Al-Sayed et al. 2019).

Therapy with Ag-NPs green, which was created from the extract of *Moringa oliefera* leaves, might shield cells from oxidative stress-related harm, death, and dysfunction. This may be explained by the fact that Nano-extract can protect cells by regulating membrane permeability, preventing glutathione depletion, and inhibiting peroxidation reactions. The Nano-extract restored the antioxidant profile by preventing peroxidation processes and the production of ROS in colinic cells as demonstrated by its capacity to quench and scavenge free radical production, which is supported by Shousha et al. (2019). Also, AntoCordeliaTA and Ping's (2017) findings, which showed that the antioxidant potential of *Moringa oliefera* leaves extract increased after integrating Ag-NPs, corroborated our findings. The increased antioxidant activity may be attributed to the antioxidant functional groups' capacity to adhere to Ag-NP surfaces.

CONCLUSIONS

This the first study for using COI gene sequences in the detection of genotoxicity, which caused by acrylamide. Our results indicated the sensitivity of this gene for exposure to acrylamide which effect on the genetic structure and cause a great of mutations in the studied rats. The present study showed also the protective role of silver nanoparticles derived from *Moringa oliefera* leaves against toxic effects of ACR.

Supplementary materials

Not applicable.

Author contributions

Conceptualization, L.E.M.D.; methodology, L.E.M.D. and A.H.Y.A; software, L.E.M.D.; validation, L.E.M.D. and N.A.O; formal analysis, L.E.M.D.; investigation, L.E.M.D.; data curation, L.E.M.D.; writing-original draft preparation, L.E.M.D.; writing-review and editing, L.E.M.D. and K.E.; visualization, L.E.M.D.; supervision, L.E.M.D. and K.E.; All authors have read and agreed to the published version of the manuscript.

Funding statement

Not applicable.

Institutional Review Board Statement

Not applicable.

Informed Consent Statement

Not applicable.

Data Availability Statement

All of the data is included in the article

Acknowledgments

Not applicable.

Conflict of interest

The authors declared that present study was performed in absence of any conflict of interest.

REFERENCES

Abdel-Rahman LH, Al-Farhan BS, El-ezz A, Sayed AE, Zikry MM, Abu-Dief AM. 2022. Green Biogenic Synthesis of Silver Nanoparticles Using Aqueous Extract of *Moringa Oleifera:* Access to a Powerful Antimicrobial, Anticancer, Pesticidal and Catalytic Agents. Journal of Inorganic and Organometallic Polymers and Materials, 32(4), 1422-1435.

Aboulthana WM, Shousha WG, Essawy EAR, Saleh MH, Salama AH. 2021. Assessment of the Anti-Cancer Efficiency of Silver *Moringa oleifera* Leaves Nano-extract against Colon Cancer Induced Chemically in Rats. Asian Pacific Journal of Cancer Prevention, 22(10), 3267-3286

Ahn JS, Castle L, Clarke DB, Lloyd AS, Philo MR, Speck DR. 2002. Verification of the findings of acrylamide in heated foods. Food Additives and Contaminants, 19(12), 1116-24.

Akaneya Y, Jiang B, Tsumoto T. 2005.RNAi-induced gene silencing by local electroporation in targeting brain region. Journal of Neurophysiology, 93(1), 594–602.

Al-Sayed E, Abdel-Daim MM, Khattab MA. 2019. Hepatoprotective activity of praecoxin A isolated from Melaleuca ericifolia against carbon

tetrachloride-induced hepatotoxicity in mice. Impact on oxidative stress, inflammation, and apoptosis. Phytotherapy Research, 33(2), 461-470.

Al-Serwi RH, Ghoneim FM. 2015. The impact of vitamin E against acrylamide induced toxicity on skeletal muscles of adult male albino rat tongue: Light and electron microscopic study. Journal of Microscopy and Ultrastructure, 3(3), 137-147.

AntoCordeliaTA D, Ping HH. 2017. Investigation of Green Synthesized Silver Nanoparticles Using Aqueous Leaf Extract of Artemisia Argyi for Antioxidant and Antimicrobial Potentials. International Journal of Pharmaceutical Quality Assurance 8(04), 190-199.

Baskar G, Aiswarya R. 2018. Overview on mitigation of acrylamide in starchy fried and baked foods. Journal of the Science of Food and Agriculture, 98(12), 4385–4394.

Bo L, Liu Y, Jia S, Liu Y, Zhang M, Li S, Zhao X, Sun C. 2018. Metabonomics analysis of quercetin against the nephrotoxicity of acrylamide in rats. Food and Function, 9(11), 5965–5974.

Brandon MC, Lott MT, Nguyen KC, Spolim S, Navathe SB, Baldi P, Wallace DC. 2005.MITOMAP: a human mitochondrial genome database--2004 update. Nucleic Acids Research, 33(Database issue), D611–D613.

Charron S, Duong C, Ménard A, Roy J, Eliopoulos V, Lambert R, Deng AY. 2005.Epistasis, not numbers, regulates functions of clustered Dahl rat quantitative trait loci applicable to human hypertension. Hypertension, 46(6), 1300–1308.

Chen D, Wang MW. 2005.Development and application of rodent models for type 2 diabetes. Diabetes, Obesity and Metabolism, 7(4), 307–317.

Dimauro S, Schon EA. 2003. Mitochondrial respiratory-chain diseases. The New England Journal of Medicine, 348, 2656-2668.

Drury RA, Wallington EA, Cancerson R. 1976. Carlton's Histopathological Techniques, Oxford University Press, Oxford**,** UK, 4th edition.

El-Bohi KM, Moustafa GG, El sharkawi NI, Sabik LME. 2011. Genotoxic effects of acrylamide in adult male Albino rats liver. Journal of American Science,7(1),1097-1108.

Exon JH. 2006. A review of the toxicology of acrylamide. Journal of Toxicology and Environmental Health. Part B, Critical Reviews, 9(5), 397–412.

Ezejindu DN, Udemezue OO, Chinweife KC. 2014. Hepatoprtective effects of Moringaoleifera extract on liver of wistar rats. International Journal of Research in Medical and Health Sciences, 3(5), 23-27.

Fahey JW. 2005.*Moringa oleifera*: a review of the medical evidence for its nutritional, therapeutic, and prophylactic properties. Part 1. Trees for Life Journal, 1(5): 1-15.

Fernández-Silva P, Enriquez JA, Montoya J. 2003.Replication and transcription of mammalian mitochondrial DNA. Experimental Physiology, 88(1), 41–56.

Finsterer J. 2004.Mitochondriopathies. European Journal of Neurology, 11(3), 163–186.

Gawesh ES, Elshoura AI, Abbas M. 2021.Protective Effect of Cinnamon and Ginger on Acrylamide Induced Hepatotoxicity in Adult Male Albino Rats. International Journal of Medical Arts, 3(1), 1136-1144.

Ghosh N, Paul S, Basak P. 2014. Silver Nanoparticles of Moringa oleifera - green synthesis, characterisation and its antimicrobial efficacy. Journal of Drug Delivery and Therapeutics, 4(3-s), 42-46.

Giles RE, Blanc H, Cann HM, Wallace DC. 1980.Maternal inheritance of human mitochondrial DNA. Proceedings of the National Academy of Sciences of the United States of America, 77(11), 6715–6719.

Ingman M, Kaessmann H, Pääbo S, Gyllensten U. 2000.Mitochondrial genome variation and the origin of modern humans. Nature, 408(6813), 708–713.

Jamshidi K. 2015.Acrylamide - induced acute nephrotoxicity in Rats. International Journal of Scientific Research in Science and Technology, 1(5), 286-293.

Kadawathagedara M, Botton J, de Lauzon-Guillain B, Meltzer HM, Alexander J, Brantsaeter AL, Haugen M, Papadopoulou E. 2018. Dietary acrylamide intake during pregnancy and postnatal growth and obesity: Results from the Norwegian Mother and Child Cohort Study (MoBa). Environment International, 113, 325–334.

Khalifa MA, Younes M, Ghazy A. 2018. Cytochrome b shows signs of adaptive protein evolution in Gerbillus species from Egypt. The Journal of Basic and Applied Zoology, 79, 1-8.

Kosakyan A, Heger TJ, Leander BS, Todorov M, Mitchell EA, Lara E. 2012.COI barcoding of Nebelid testate amoebae (Amoebozoa: Arcellinida): extensive cryptic diversity and redefinition of the Hyalospheniidae Schultze. Protist, 163(3), 415–434.

Kumar S, Stecher G, Tamura K. 2016. MEGA7: Molecular evolutionary genetics analysis version 7.0 for bigger datasets. Molecular Biology and Evolution, 33(7), 1870-1874.

LoPachin RM. 2004.The changing view of acrylamide neurotoxicity. Neurotoxicology, *25*(4), 617–630.

LoPachin RM, Barber DS, He D, Das S. 2006. Acrylamide inhibits dopamine uptake in rat striatal synaptic vesicles. Toxicological Sciences, 89(1), 224–234.

Lynch M, Koskella B, Schaack S. 2006.Mutation pressure and the evolution of organelle genomic architecture. Science, 311(5768), 1727–1730.

Mahmood KT, Mugal T, Haq IU. 2010.*Moringa oleifera*: a natural gift-A review.Journal of Pharmaceutical Sciences and Research, 2(11), 775-781.

Malathi R, Chandrasekar S, Sivakumar D. 2018.

Assessment of toxicity study of ethanolic extract and synthesized silver nanoparticles of *Moringa concanensis* Nimmo leaves using wister albino rats. *International* Journal of Current Research in Life Sciences, 7(3), 1250-1254.

Manjanatha MG, Aidoo A, Shelton SD, Bishop ME, McDaniel LP, Lyn-Cook LE, Doerge DR. 2006.Genotoxicity of acrylamide and its metabolite glycidamide administered in drinking water to male and female Big Blue mice. Environmental and Molecular Mutagenesis, 47(1), 6–17.

Mason PA, Lightowlers RN. 2003.Why do mammalian mitochondria possess a mismatch repair activity? FEBS Letters, 554(1-2), 6–9.

Ng DP, Krolewski AS. 2005.Molecular genetic approaches for studying the etiology of diabetic nephropathy. Current Molecular Medicine, 5(5), 509–525.

Prakash D, Singh BN, Upadhyay G. 2007.Antioxidant and free radical scavenging activities of phenols from onion (Allium cepa). Food Chemistry,102, 1389-1393.

Rahangadale S, Kurkure N, Prajapati B, Hedaoo V, Bhandarkar AG. 2012.Neuroprotective effect of vitamin e supplementation in wistar rat treated with acrylamide. Toxicology International, 19(1), 1–8.

Ramaswamy M, Solaimuthu C, Duraikannu S. 2019. Antiarthritic activity of synthesized silver nanoparticles from aqueous extract of Moringa concanensis Nimmo leaves against FCA induced rheumatic arthritis in rats.Journal of Drug Delivery and Therapeutics, 9(3), 66-75.

Regoli F, Nigro M, Benedetti M, Gorbi S, Pretti C, Gervasi PG, Fattorini D. 2005.Interactions between metabolism of trace metals and xenobiotic agonists of the aryl hydrocarbon receptor in the antarctic fish *Trematomus bernacchii*: environmental perspectives. Environmental Toxicology and Chemistry, 24(6), 1475–1482.

Rizk MZ, Abo-El-Matty DM, Aly HF, Abd-Alla HI, Saleh SM, Younis EA, Elnahrawy AM, Haroun AA. 2018. Therapeutic activity of sour orange albedo extract and abundant flavanones loaded silica nanoparticles against acrylamide-induced hepatotoxicity. Toxicology Reports, 5, 929–942.

Sahai V. 2012. Histological changes in liver of albino mice due to chronic administration of acrylamide. Indian Journal of Fundamental and Applied Life Science, 2(3), 51-54.

Senthilkumar R, Chandran R, Parimelazhagan T. 2014.Hepatoprotective effect of Rhodiola imbricata rhizome against paracetamol-induced liver toxicity in rats. Saudi Journal of Biological Sciences, 21(5), 409–416.

Shipp A, Lawrence G, Gentry R, McDonald T, Bartow H, Bounds J, Macdonald N, Clewell H, Allen B, Van Landingham C. 2006.Acrylamide: review of toxicity data and dose-response analyses for cancer and noncancer effects. Critical Reviews in Toxicology, 36(6-7), 481–608.

Shousha WG, Aboulthana WM, Salama AH, Saleh MH, Essawy EA. 2019.Evaluation of the biological activity of Moringa oleifera leaves extract after incorporating silver nanoparticles, in vitro study.Bulletin of the National Research Centre,43, 1-13.

Sickles DW, Sperry AO, Testino A, Friedman M. 2007.Acrylamide effects on kinesin-related proteins of the mitotic/meiotic spindle. Toxicology and Applied Pharmacology, 222(1), 111–121.

Törnqvist M. 2005.Acrylamide in food: the discovery and its implications: a historical perspective. Advances in Experimental Medicine and Biology, 561, 1–19.

Van Dijk SJ, Specht PA, Lutz MM, Lazar J, Jacob HJ, Provoost AP. 2005.Interaction between Rf-1 and Rf-4 quantitative trait loci increases susceptibility to renal damage in double congenic rats. Kidney International, 68(6), 2462–2472.

Zong NC, Li H, Li H, Lam MP, Jimenez RC, Kim CS, Deng N, Kim AK, Choi JH, Zelaya I, Liem D, Meyer D, Odeberg J, Fang C, Lu HJ, Xu T, Weiss J, Duan H, Uhlen M, Yates JR 3rd, Apweiler R, Ge J, Hermjakob H, Ping P. 2013.Integration of cardiac proteome biology and medicine by a specialized knowledgebase. Circulation Research, 113(9), 1043–1053.